High-precision half-life measurement of the β^+ decay of ^{21}Na

P. D. Shidling,[1,*] R. S. Behling,[1,2] B. Fenker,[1,3] J. C. Hardy,[1,3] V. E. Iacob,[1] M. Mehlman,[1,3] H. I. Park,[1] B. T. Roeder,[1] and D. Melconian[1,3]

[1]*Cyclotron Institute, Texas A&M University, College Station, Texas 77843-3366, USA*

[2]*Department of Chemistry, Texas A&M University, College Station, Texas 77843-3012, USA*

[3]*Department of Physics and Astronomy, Texas A&M University, College Station, Texas 77843-4242, USA*

(Received 19 February 2018; published 27 July 2018)

The β^+ decay of ^{21}Na to ^{21}Ne is one of the four cases currently being used to determine the value of V_{ud} from nuclear mirror ($T = 1/2$) transitions. To date, published values for the half-life of ^{21}Na have not been consistent with one another. We report here a new measurement of the half-life: $22.4615 \pm 0.0039_{(stat)} \pm {}^{0.0001}_{0.0015\,(syst)}$ s. This result increases the world average of the ^{21}Na half-life by 0.0048 s and reduces the uncertainty by a factor of 1.5.

DOI: 10.1103/PhysRevC.98.015502

I. INTRODUCTION

Precision β-decay measurements in nuclei have a long history of testing discrete symmetries in the weak interaction, and they continue to give valuable information on the fundamental coupling of charged fermions to weak bosons. The scientific motivation for such measurements is to test predictions of the standard model and search for experimental deviations that could be indications of new physics. One way to probe the standard model is to determine the precise value of V_{ud}, the up-down element of the Cabbibo–Kobayashi-Maskawa (CKM) matrix, and test the unitarity of CKM matrix.

The most stringent test of CKM unitarity comes from the sum of squares of the top-row elements:

$$|V_{ud}|^2 + |V_{us}|^2 + |V_{ub}^2| = 1. \tag{1}$$

The value of V_{ud} is obtained from weak decay processes involving the lightest quarks and, currently, its most precise determination comes from the fourteen nuclear superallowed $0^+ \rightarrow 0^+$ pure-Fermi transitions [1–4]. To determine V_{ud} from these transitions, measurements of their ft values combined with a few calculated terms to account for radiative and nuclear-structure dependent effects are required. The ft value for a given transition depends on three measured quantities: the half-life ($t_{1/2}$), the branching ratio (BR), and the total transition energy (Q_{EC}).

A different set of nuclear transitions has also been considered for determining the V_{ud} value [5,6]. These nuclear transitions are mixed Fermi and Gamow–Teller transitions between $T = 1/2$ isospin doublets. They are mediated by both the vector and axial-vector component of the weak interaction. Thus the extraction of V_{ud} from one of these transitions requires more than the ft value: An additional angular-correlation coefficient must be measured to separate the axial-vector contribution from the vector one. Neutron decay is another source to determine the value of V_{ud}. It also involves both the vector and the axial-vector interactions so that the determination of V_{ud} requires the analysis of at least two observables [7].

For mixed Fermi-Gamow–Teller transitions, a "corrected" $\mathcal{F}t$ value, defined in terms of the measured ft value, can be related to V_{ud} by

$$\begin{aligned}\mathcal{F}t &\equiv f_V t(1+\delta_R')\left(1+\delta_{NS}^V-\delta_C^V\right)\\ &= \frac{K}{G_F^2 V_{ud}^2}\frac{1}{C_V^2\left|M_F^0\right|^2\left(1+\Delta_R^V\right)\left[1+\left(\frac{f_A}{f_V}\right)\rho^2\right]},\end{aligned} \tag{2}$$

where $K/(\hbar c)^6 = 2\pi^3 \ln 2\hbar/(m_e c^2)^5 = 8120.278(4) \times 10^{-10}$ GeV^{-4} s, G_F is the Fermi constant, where $G_F/(\hbar c)^3 = 1.16637(1) \times 10^{-10}$ GeV^{-2}, and $C_V = 1$. The parameters δ_R', δ_{NS}^V, Δ_R^V, and δ_C^V are the radiative and isospin-symmetry-breaking correction terms calculated for the vector current; f_V and f_A are statistical rate functions for the vector and axial-vector currents, respectively; M_F^0 is the symmetry-limit Fermi matrix element, which takes the value 1 for $T = 1/2$ mirror transitions; and ρ is the Fermi-Gamow–Teller mixing ratio, which can be obtained from a measurement of any one of the angular-correlation parameters ($a_{\beta\nu}$, A_β, B_ν) [6].

For convenience in analyzing $T = 1/2$ decays, Naviliat–Cuncic and Severijns [6] defined the quantity

$$\mathcal{F}t_0 \equiv \mathcal{F}t\ C_V^2\ \left|M_F^0\right|^2\left[1+\left(\frac{f_A}{f_V}\right)\rho^2\right], \tag{3}$$

which collects together all the terms associated with a particular decay. Thus,

$$V_{ud}^2 = \frac{K}{\mathcal{F}t_0\ G_F^2\left(1+\Delta_R^V\right)} \tag{4}$$

and, due to conservation of the vector current, the $\mathcal{F}t_0$ values for $T = 1/2$ mirror transitions should all be the same. They should also be exactly double the $\mathcal{F}t$ values obtained for superallowed $0^+ \rightarrow 0^+$ decays.

*pdshidling@tamu.edu

The decay of ^{21}Na is one of the four cases of $T = 1/2$ nuclear mirror transitions currently being used to determine a value for V_{ud} to compare with the more precise value obtained from the superallowed $0^+ \rightarrow 0^+$ β transitions, so its ft-value uncertainty is critical. The largest contributor to that uncertainty is its branching ratio but the contribution from its half-life is also significant. Moreover, the half-life uncertainty is hampered by the fact that the two most recent half-life measurements—in 2015 [8] and 2017 [9]—are not consistent with one another. In this paper, we present a precise half-life measurement for ^{21}Na aimed at resolving this discrepancy.

II. EXPERIMENT

We performed the half-life measurement of ^{21}Na at the Cyclotron Institute of Texas A&M University by using a 4π continuous gas-flow proportional counter [10] and a fast tape-transport system. We produced ^{21}Na via an inverse kinematics reaction (fusion-evaporation reaction) by directing a primary beam of ^{22}Ne ($E_{beam} = 25$ MeV/u) onto a 1.6 atm H_2 gas target cooled to liquid nitrogen temperature. The fully stripped reaction products exiting the target cell entered the momentum achromat recoil spectrometer (MARS) [11–13], where they were analyzed and purified according to their mass-to-charge ratio $m/q = m/Ze$.

A high-purity beam of ^{21}Na was essential for us to perform a high-precision half-life measurement and to reduce the contribution of systematic effects in the final uncertainty attached to the half-life. The settings of MARS were adjusted to focus ^{21}Na and minimize potential impurities, with the aid of a 16-strip position-sensitive silicon detector (PSSD) of 300 μm thickness and active area of 5×5 cm^2, which we inserted initially at the MARS focal plane. The reaction products were identified according to their position and energy-loss in the strip detector. After the settings of MARS had been optimized, the focal-plane acceptance slits were set 18 mm apart. This limited the dominant contaminants, ^{19}Ne (which has a similar half-life to that of ^{21}Na), ^{17}F, and ^{15}O, to 0.1%. Figure 1 shows the two-dimensional plot of energy loss vs position as obtained with the PSSD in the MARS focal plane.

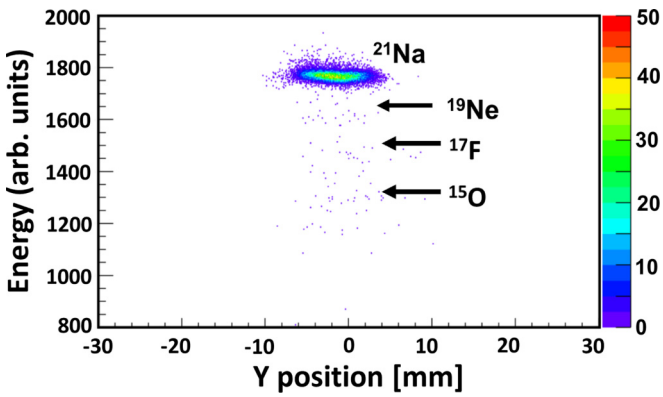

FIG. 1. Two-dimensional plot of energy-loss versus position in the PSSD at the MARS focal plane after the spectrometer had been optimized for ^{21}Na production and the acceptance slits set to +10 and −8 mm.

During the course of the experiment, the PSSD at the MARS focal plane was inserted twice a day to check the beam purity; no change in the purity level was observed at any time.

The purified ^{21}Na beam exited the vacuum system through a 51-μm-thick Kapton foil and passed through a 0.3-mm-thick BC-404 plastic scintillator, which counted the number of ions. The beam then passed through a stack of aluminum degraders, and finally was implanted into the 76-μm-thick aluminized Mylar tape of our fast tape-transport system.

Before starting the half-life measurement, we took advantage of the fact that the range of lighter ions (^{19}Ne, ^{17}F, and ^{15}O) in the Al degrader are longer that of the ^{21}Na ions. We optimized the Al degrader thickness by measuring the ^{21}Na activity collected in the mylar tape as a function of the Al thickness in steps of 12.7 μm, ranging from 63.5 to 139 μm. In this way, we could select the degrader thickness that left all the ^{21}Na implanted in the Mylar tape, while allowing other impurities (^{19}Ne, ^{17}F, and ^{15}O) to pass entirely through the tape. The energy of ^{19}Ne, ^{17}F, and ^{15}O at the exit of optimized Al degrader thickness were 120 M, 150 M, and 160 MeV, respectively, which corresponds to the range of 102, 184, and 270 μm in the Mylar material. The range calculations were carried out by using SRIM [14] and LISE++ [13] software packages. Thus, the combination of m/q selectivity in MARS and range selectivity in the degrader led to implanted ^{21}Na samples that were greater than 99.98% pure.

Each source of ^{21}Na was prepared by implantation of the ^{21}Na beam into a section of aluminized Mylar tape for 20 s. The beam was then turned off and our tape-transport system moved the sample in 180 ms to a well-shielded detector station consisting of a high-efficiency 4π proportional gas counter. The decay positrons were then observed for 450 s, which is equal to twenty half-lives. These collect-move-detect cycles were computer controlled and their timing was continuously monitored online. This cycle was repeated until the desired statistics had been accumulated. The background rate in the gas counter was about 0.6 counts/s, which is 4 orders of magnitude lower than the initial count rate for each collected sample.

The gas counter and data-acquisition system are the same ones used in a number of previous precision measurements of the half-lives of superallowed β-emitters performed at Texas A&M University (e.g., Refs. [10,15,16]). In short, the pre-amplified signals from the gas counter are processed through a fast filter amplifier with a high gain (×500). These amplified signals are sent to a discriminator with a low threshold (150–250 mV), its output signal being split and sent to two fixed-width and nonextending gate generators, which established two dominant dead times. Finally, the two processed signals are multiscaled into separate 500-channel time spectra that we designate to be from multiscalers A and B.

The total measurement was split into 21 runs, each with a different combination of experimental conditions selected from: three discriminator threshold settings (150, 200, and 250 mV), two combinations of dead times (4 and 6 μs; 3 and 8 μs), and four detector bias voltages within the detector's plateau region (2600, 2650, 2700, and 2750 V). Finally, a background measurement was performed for which all conditions were the same as for normal data taking except that the tape-move feature was disabled.

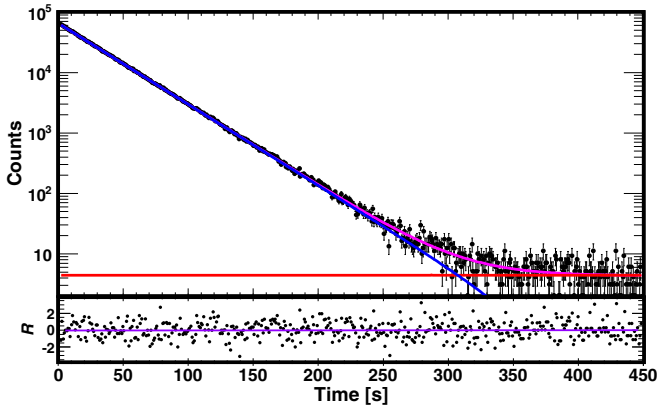

FIG. 2. Typical dead-time-corrected summed decay curve obtained from a single run with residuals ($R = \frac{\text{data-fit}}{\sqrt{\text{fit}}}$) shown at the bottom of the spectrum. The fitting function accounts for a constant background (red) and an exponential corresponding to the decay of ^{21}Na (blue). The total fit decay curve is shown by a magenta line. The reduced χ^2 of the fit is 1.10.

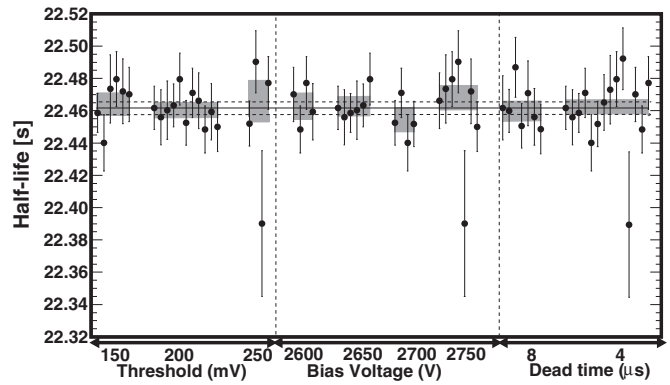

FIG. 3. Test for any systematic bias in the ^{21}Na half-life measurement due to changes in three different detection parameters. Results from all 21 runs appear three times, grouped on the left by the threshold setting, in the middle by bias, and on the right by dead time. In all cases, the gray bands represent the $\pm\sigma$ limits of the average half-life for a given condition. The average value for all the runs appears as a solid horizontal line, with the corresponding dashed lines as the statistical uncertainty limits. The reduced χ^2 for the average is 0.82.

III. ANALYSIS AND RESULTS

A. Data processing

The selection of data for final analysis was made according to two criteria. First, cycles with too few counts (<10 000) were rejected, since evidently there had been little or no primary beam from the cyclotron during that cycle's collection period. Second, cycles were rejected which had a low ratio between the number of βs recorded in each cycle and the corresponding number of heavy ions recorded in the BC-404 plastic scintillator at the exit of MARS. For these cycles the tape had not stopped at the center of the proportional counter. Together, these filters removed about 18% of the recorded cycles. After all filters we were left with 5.5×10^7 decays.

The accepted cycles from each run were first corrected channel-by-channel for dead time. Next, the cycles constituting each run were summed into two decay curves, one for each imposed dead time. We fit the summed decay curves using the program we wrote based on the Levenberg–Marquardt algorithm for χ^2 minimization assuming the data obey Poisson rather than Gaussian statistics [17]. This is the "summed" method described in Ref. [18]. Figure 2 shows a typical summed decay curve of the dead-time-corrected data obtained from a single run. The fit function contained a constant background and an exponential corresponding to the decay of ^{21}Na. The final half-life for ^{21}Na was derived from the average of the results from the 21 separately analyzed runs.

In addition, we performed a cycle-by-cycle analysis, in which the data were fit cycle-by-cycle and the half-life was derived by taking the weighted average of all fitted cycles. The value of half-life from this analysis method was in good agreement with the one obtained from the first method, so we only use the summed fit in what follows.

B. Half-life determination

As mentioned in Sec. II, we recorded 21 runs, each with a different combination of detector settings, in order to test for potential systematic effects that could contribute to the uncertainty in the half-life. In Fig. 3 we plot the half-lives obtained from each run grouped together differently in each part of the figure to illustrate the effects of changing one of the three pertinent experimental parameters: bias voltage, discriminator setting, and imposed dominant dead time. All the results were taken from multiscaler A except for the group with 8 μs dead time, which came from multiscaler B. The solid and dashed lines correspond to the overall average half-life with its statistical uncertainty. No statistically significant dependence of the half-life on any of the three detection parameters is apparent in the figure. This conclusion is confirmed by the reduced χ^2 for the overall average half-life, which is 0.82.

As another systematic check for possible count-rate-dependent effects or the presence of short-lived impurities, we removed up to 110 s (122 channels) from the beginning of the counting period in steps of 1 s for the first 4 s and later in steps of 5 and 10 s. We refitted the remainder after each removal. From Fig. 4 it is clear that, within statistics, the derived half-life was also stable against these changes.

We also tested for rate-dependent effects arising from the initial count rate of each cycle. All of the cycles were collected into five different groups based on their initial count rate, ranging from 0 to 2 kHz, 2 to 4 kHz, 4 to 6 kHz, 6 to 8 kHz, and above 8 kHz. The data from all 21 runs were included. The half-lives obtained from the five groups were all statistically consistent with one another.

With no evident dependence on counting parameters revealed by these tests, our final average value for the ^{21}Na half-life is 22.4615(39) s with a reduced χ^2—as already noted—of 0.82. At this stage, the uncertainty is purely statistical.

We turn now to systematic uncertainties that arise from undetected contaminants possibly affecting our decay spectra. In Sec. II, we presented data and calculations as evidence that ^{19}Ne, which has a half-life similar to that of ^{21}Na, was

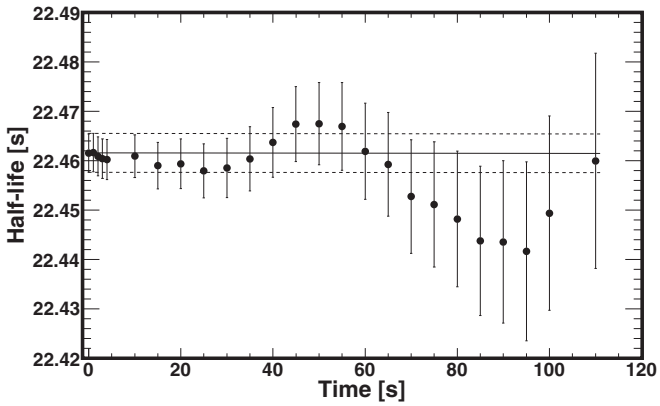

FIG. 4. Test of short-lived impurities or possible rate-dependent effects. Each point is the result of a separate fit to the data, the abscissa for each point representing the time period at the beginning of the counting cycle for which the data were omitted from that particular fit. The solid and dashed lines corresponds to the average half-life and statistical uncertainty for the full data set. Note that the last point on the graph represents only ∼3% of the total counts recorded.

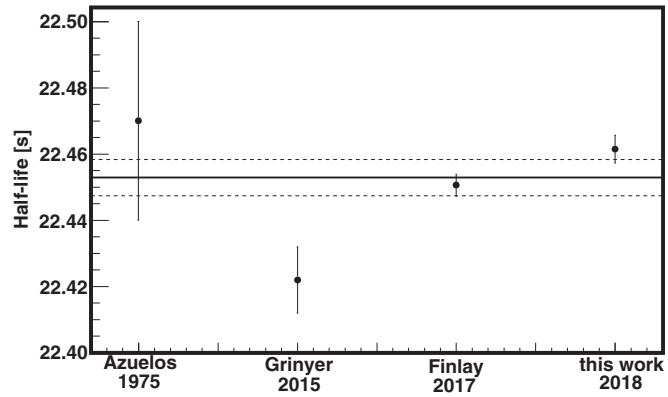

FIG. 5. World-average half-life of ^{21}Na. Shown are the measurements from Azuelos: [22], Grinyer: [8], Finlay: [9] and this work. Results which are more than ten time less precise as compared with the value reported in this work have not been considered. See text for further discussion. The weighted average of all results is 22.4528(52) s, where the uncertainty has been increased by $\sqrt{\chi^2/3} = 2.2$ to account for the inconsistency of the results.

completely absent from our collected samples. We conservatively refitted our decay data assuming that 20% of the total ^{19}Ne impurity observed at the MARS focal plane (see Fig. 1) was actually implanted in the tape. This would mean that the number of ^{19}Ne atoms deposited in the tape each cycle was 0.02% of the number of ^{21}Na atoms deposited. Under this condition, the increase in the fitted half-life for ^{21}Na was a mere 0.0001 s, much less than the statistical uncertainty of 0.0039 s. This result appears in the uncertainty budget recorded in Table I.

Another possible contributor to the decay spectra is ^{66}Cu, originating from neutron activation of the copper housing of the 4π proportional gas counter [19]. Neutron activation of stable isotopes of copper (^{63}Cu and ^{65}Cu) can produce ^{64}Cu and ^{66}Cu, respectively. The former has a half-life of 12.7 h and would have no affect on our result, but the latter, with $t_{1/2} = 5.12$ min., could certainly have an impact. If it were present, although, we would expect to have seen it in the dedicated background run, which was recorded with the same conditions as for normal data taking except that the tape-move feature was disabled. No decay pattern was evident in that spectrum but, nevertheless, we fit it with a constant background plus a component with a 5.12-min half-life and obtained a statistical upper limit on its possible presence. We then introduced this upper limit into the fitting function used to determine the ^{21}Na half-life. This results in the asymmetric uncertainty listed for ^{66}Cu in Table I.

With both statistical and systematic uncertainties incorporated, our final result is

$$t_{1/2}(^{21}\mathrm{Na}) = 22.4615 \pm 0.0039_{\text{(stat)}} \pm {}^{0.0001}_{0.0015}\,\text{s}_{\text{(syst)}}. \quad (5)$$

TABLE I. Error budget for the ^{21}Na half-life measurement.

Source	Uncertainty (ms)
Statistical	±3.9
Systematics:	
potential ^{19}Ne contaminant	$^{+0.1}_{-0.0}$
potential ^{66}Cu contaminant	$^{+0.0}_{-1.5}$
Total systematic	$^{+0.1}_{-1.5}$
Total uncertainty	$^{+3.9}_{-4.2}$

C. Comparison with previous results

Previous measurements of the ^{21}Na lifetime obtained are $t_{1/2} = 23.0 \pm 0.2$ s [20], 22.55 ± 0.10 s [21], 22.47 ± 0.03 s [22], 22.422 ± 0.010 s [8], and 22.4506 ± 0.0033 s [9]. Of these five results, the first two, from 1958 and 1974, have uncertainties that are greater than 10 times the most precise measurement and consequently they do not contribute to the world average. We will not consider them further.

The other, more precise, measurements are shown, along with the present result, in Fig. 5. Our half-life is in agreement with the value obtained by Azuelos *et al.* [22], but disagrees with the other two results, which in fact do not agree with one another.

The measurements by Grinyer *et al.* [8] and Finlay *et al.* [9] both used sources obtained by stopping all beam-produced atoms, then ionizing them and passing them through an isotope separator, which was set to accept only ions with $A/q = 21$. With such an arrangement, both systems could, in principle, have produced other $A = 21$ isobars with $q = +1$, in addition to ^{21}Na. By using a surface-ionization ion source, Finlay *et al.* ensured that higher charge states were not created in their experiment, but Grinyer *et al.*, who used a FEBIAD ion source, could also have deposited doubly charged ions with $A = 42$. To rule out the presence of such impurities, both sets of authors employed an HPGe detector placed close to the collected ^{21}Na source, arguing that any impurity would be revealed by the observation of γ rays characteristic of its decay. The sensitivity of this γ-ray technique is both limited and highly variable,

being considerably less efficient than the β detection used in the half-life measurement and being completely dependent on what fraction of the impurity's β decay actually leads to emission of a γ ray.

In their publication [8], Grinyer *et al.* do not show a γ-ray spectrum but state that they see evidence for $^{42}K^{2+}$, presumably through observation of the 1524.6 keV γ ray, produced in 18.1% of ^{42}K decays. They further state that they see no evidence of $A = 21$ isobars "such as ^{21}O, ^{21}F, and ^{21}Mg," although they set no upper limits on their possible presence. The identified isotope, ^{42}K, has too long a half-life ($t_{1/2} = 12.4$ hr) to be of concern, but ^{21}O (3.42 s), ^{21}F (4.16 s), and even ^{42}Cl (6.8 s) all have half-lives which, if not accounted for in data analysis, could lead to too short a half-life being obtained for ^{21}Na. This is a plausible explanation for the $\sim$0.15% ($>3\sigma$) discrepancy between their result and the two more recent measurements.

The half-life measured by Finlay *et al.* [9] is much closer to our result, differing by only $\sim$0.05%, or 10 ± 5 ms. In their publication, they do show their γ-ray spectrum, from which they set a limit on possible ^{21}F contamination. The only unique signature of ^{21}F would be a 1395 keV γ ray that occurs in 15% of its decays. There is significant background in that region of their spectrum, but the authors nevertheless set a limit on the possible activity of ^{21}F at 5.6×10^{-5} relative to that of ^{21}Na. That tiny amount would have very little influence on the half-life obtained for ^{21}Na but if it were actually larger by, say, a factor of 10 (which would still be a small contamination), then the discrepancy with our result would be removed.

In our measurement, we are unaffected by $A = 21$ isobars since, as explained in Sec. II, the ions passing through the MARS spectrometer were fully stripped, thus being spatially separated according to their A/Z ratio. The nearest two isobars have A/Z ratios that differ by 10% from that of ^{21}Na and, consequently, are cleanly removed. We determined a limit on our only possible beam-produced contaminant, ^{19}Ne, based on direct observation (see Fig. 1). It has a negligible effect (see Table I). Note that our methodology for identifying and characterizing contaminants is the only measurement of ^{21}Na which is not based on a γ spectrum.

We have evaluated the world average from the four results that appear in Fig. 5; these are the only results that meet the criterion [4,5] that their uncertainties must be less than ten times the uncertainty of the most precise measurement. Under these conditions, the average is

$$t_{1/2} = 22.4528 \pm 0.0055 \text{ s}, \tag{6}$$

which is higher by 0.0048 s and is a factor of 1.5 more precise than the previous world-average value quoted in Ref. [9]. However, both uncertainties are heavily influenced by the disagreement among the contributing measurements. A relatively large scale factor, which is the square-root of the reduced χ^2 of the derived average, has been applied in both cases: 1.7 in the previous world average and 2.2 in the new one. It can be noted that the largest contributor to this factor is the result from Grinyer *et al.* [8]. If it were removed, the half-life average would become 22.4549 ± 39 s, which includes a scale factor of only 1.5.

TABLE II. Input data used to determine the value of V_{ud} for ^{21}Na.

$t_{1/2}$	22.4528(55) s	This work
BR	95.235(69)%	Ref. [5]
Q_{EC}	3547.11(9) keV	Ref. [23]
f_V	170.815(27)	Ref. [23]
δ'_R	1.514(15)%	Ref. [5]
$\delta_C^V - \delta_{NS}^V$	0.41(3)%	Ref. [5]
Δ_R^V	2.361(38)%	Refs. [5,25]
ρ	−0.7136(72)	Refs. [6,24]
$\mathcal{F}t$	4075.2(34) s	This work
$\mathcal{F}t_0$	6188.0(43) s	This work

IV. EXTRACTION OF V_{ud}

We calculate the $\mathcal{F}t$ value for ^{21}Na by taking its branching ratio to be BR = 95.235(69)% from the survey of Ref. [5], its Q_{EC} value, 3547.11(9) keV, from a recent measurement with a Penning trap [23], and its world-average half-life from Eq. (6). The result is

$$\mathcal{F}t = 4075.2 \pm 3.4 \text{ s}. \tag{7}$$

This, combined with the value of $\rho = -0.7136(72)$ from Refs. [6,24], leads to

$$\mathcal{F}t_0 = 6188 \pm 43 \text{ s} \tag{8}$$

for ^{21}Na, a value that is $\sim$0.2% lower than the one quoted 10 years ago in the survey by Naviliat–Cuncic and Severijns [6]. The data used to determine the value of V_{ud} for ^{21}Na is summarized in Table II.

From this result, we calculate that

$$|V_{ud}| = 0.9708 \pm 0.0035, \tag{9}$$

when derived from the ^{21}Na data alone. This value for V_{ud} is statistically consistent with the more-precise value for V_{ud} determined for the superallowed $0^+ \rightarrow 0^+$ transitions: viz. 0.9742(2) [4].

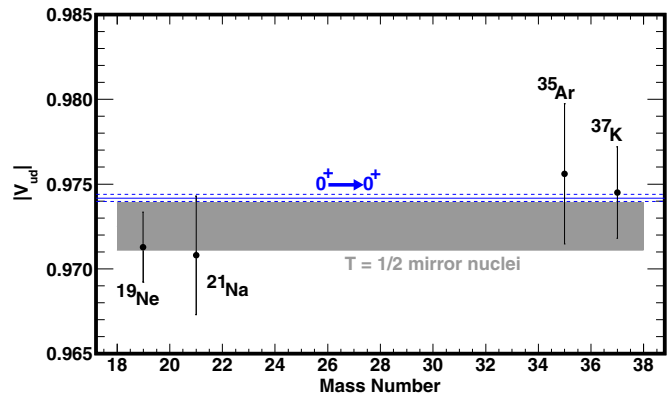

FIG. 6. V_{ud} values for $T = 1/2$ mirror nuclear decays. The results are taken from the latest survey of world data [5,6] updated by new half-life results for ^{19}Ne [26–29] and ^{37}K [18] and a new ρ for ^{37}K [30]. The ^{21}Na V_{ud} value is the one that appears in Eq. (9).

In Fig. 6 we plot V_{ud} values for the four most precisely measured nuclear mirror transitions. Evidently, they are statistically consistent with one another and with the result from $0^+ \rightarrow 0^+$ superallowed decays [4].

V. CONCLUSION

Our purpose in making this measurement of the ^{21}Na half-life was to resolve the discrepancy between the results from two recent measurements, one quoting 0.045% precision [8] and the other 0.015% [9], which differed from one another by 0.13%, or 29 ± 11 ms. This 3σ discrepancy has led to a scaled-up uncertainty on the world average, and begged for some resolution of the conflict. In the end, our new result strongly disfavors the half-life measured by Grinyer *et al.* [8] but unfortunately does not fully agree with Finlay *et al.* [9]. We propose that undetected impurities in the previous measurements could account for the discrepancies, but obviously that is only speculation.

In any case, the new world average value for the half-life given in Eq. (6) is quoted to $\pm 0.025\%$, which is quite sufficient for the time being. The new $\mathcal{F}t$ value [Eq. (7)] is now limited in precision by the 95.235(69)% ground-state branching ratio, which has a three-times-larger uncertainty of $\pm 0.072\%$. More important still, the uncertainties of $\mathcal{F}t_0$ [Eq. (8)] and V_{ud} [Eq. (9)] are dominated by the $\pm 1.0\%$ uncertainty associated with the value of ρ, which derives from a difficult correlation measurement for the transition [24]. Any further improvement in V_{ud} precision must be sought from an improved correlation measurement.

ACKNOWLEDGMENTS

We are grateful to the support staff of the Cyclotron Institute for providing the primary beam. This work was supported by the US Department of Energy Grant No. DE-FG02-93ER40773 and Early Career Award ER41747; as well as by the Welch Foundation under Grant No. A-1397.

[1] J. C. Hardy and I. S. Towner, Phys. Rev. Lett. **94**, 092502 (2005).
[2] J. C. Hardy and I. S. Towner, Phys. Rev. C **71**, 055501 (2005).
[3] J. C. Hardy and I. S. Towner, Phys. Rev. C **79**, 055502 (2009).
[4] J. C. Hardy and I. S. Towner, Phys. Rev. C **91**, 025501 (2015).
[5] N. Severijns, M. Tandecki, T. Phalet, and I. S. Towner, Phys. Rev. C **78**, 055501 (2008).
[6] O. Naviliat-Cuncic and N. Severijns, Phys. Rev. Lett. **102**, 142302 (2009).
[7] M. A.-P. Brown, E. B. Dees, E. Adamek, B. Allgeier, M. Blatnik, T. J. Bowles, L. J. Broussard, R. Carr, S. Clayton, C. Cude-Woods, S. Currie, X. Ding, B. W. Filippone, A. García, P. Geltenbort, S. Hasan, K. P. Hickerson, J. Hoagland, R. Hong, G. E. Hogan, A. T. Holley, T. M. Ito, A. Knecht, C.-Y. Liu, J. Liu, M. Makela, J. W. Martin, D. Melconian, M. P. Mendenhall, S. D. Moore, C. L. Morris, S. Nepal, N. Nouri, R. W. Pattie, Jr., A. Pérez Galván, D. G. Phillips, II, R. Picker, M. L. Pitt, B. Plaster, J. C. Ramsey, R. Rios, D. J. Salvat, A. Saunders, W. Sondheim, S. J. Seestrom, S. Sjue, S. Slutsky, X. Sun, C. Swank, G. Swift, E. Tatar, R. B. Vogelaar, B. VornDick, Z. Wang, J. Wexler, T. Womack, C. Wrede, A. R. Young, and B. A. Zeck, Phys. Rev. C **97**, 035505 (2018).
[8] J. Grinyer, G. F. Grinyer, M. Babo, H. Bouzomita, P. Chauveau, P. Delahaye, M. Dubois, R. Frigot, P. Jardin, C. Leboucher, L. Maunoury, C. Seiffert, J. C. Thomas, and E. Traykov, Phys. Rev. C **91**, 032501(R) (2015).
[9] P. Finlay, A. T. Laffoley, G. C. Ball, P. C. Bender, M. R. Dunlop, R. Dunlop, G. Hackman, J. R. Leslie, A. D. MacLean, D. Miller, M. Moukaddam, B. Olaizola, N. Severijns, J. K. Smith, D. Southall, and C. E. Svensson, Phys. Rev. C **96**, 025501 (2017).
[10] V. E. Iacob, J. C. Hardy, A. Banu, L. Chen, V. V. Golovko, J. Goodwin, V. Horvat, N. Nica, H. I. Park, L. Trache, and R. E. Tribble, Phys. Rev. C **82**, 035502 (2010).
[11] R. Tribble, C. Gagliardi, and W. Liu, Nucl. Instrum. Methods Phys. Res., Sect. B **56-57**, 956 (1991).
[12] R. E. Tribble, A. Azhari, C. A. Gagliardi, J. C. Hardy, A. Mukhamedzhanov, X. Tang, L. Trache, and S. J. Yennello, Nucl. Phys. A **701**, 278 (2002).
[13] O. B. Tarasov and D. Bazin, Nucl. Instrum. Methods Phys. Res., Sect. B **376**, 185 (2016).
[14] J. F. Ziegler, M. D. Ziegler, and J. P. Biersack, Nucl. Instrum. Methods Phys. Res., Sect. B **268**, 1818 (2016).
[15] V. E. Iacob, J. C. Hardy, J. F. Brinkley, C. A. Gagliardi, V. E. Mayes, N. Nica, M. Sanchez-Vega, G. Tabacaru, L. Trache, and R. E. Tribble, Phys. Rev. C **74**, 055502 (2006).
[16] H. I. Park, J. C. Hardy, V. E. Iacob, L. Chen, J. Goodwin, N. Nica, E. Simmons, L. Trache, and R. E. Tribble, Phys. Rev. C **85**, 035501 (2012).
[17] V. T. Koslowsky, E. Hagberg, J. C. Hardy, G. Savard, H. Schmeing, K. S. Sharma, and X. J. Sun, Nucl. Instrum. Methods Phys. Res., Sect. A **401**, 289 (1997).
[18] P. D. Shidling, D. Melconian, S. Behling, B. Fenker, J. C. Hardy, V. E. Iacob, E. McCleskey, M. McCleskey, M. Mehlman, H. I. Park, and B. T. Roeder, Phys. Rev. C **90**, 032501(R) (2014).
[19] V. E. Iacob, J. C. Hardy, V. Golovko, J. Goodwin, N. Nica, H. I. Park, L. Trache, and R. E. Tribble, Phys. Rev. C **77**, 045501 (2008).
[20] S. E. Arnell, J. Dubois, and O. Almén, Nucl. Phys. **6**, 196 (1958).
[21] D. E. Alburger, Phys. Rev. C **9**, 991 (1974).
[22] G. Azuelos and J. E. Kitching, Phys. Rev. C **12**, 563 (1975).
[23] M. Eibach, G. Bollen, M. Brodeur, K. Cooper, K. Gulyuz, C. Izzo, D. J. Morrissey, M. Redshaw, R. Ringle, R. Sandler, S. Schwarz, C. S. Sumithrarachchi, A. A. Valverde, and A. C. C. Villari, Phys. Rev. C **92**, 045502 (2015).
[24] P. A. Vetter, J. R. Abo-Shaeer, S. J. Freedman, and R. Maruyama, Phys. Rev. C **77**, 035502 (2008).
[25] W. J. Marciano and A. Sirlin, Phys. Rev. Lett. **96**, 032002 (2006).
[26] S. Triambak, P. Finlay, C. S. Sumithrarachchi, G. Hackman, G. C. Ball, P. E. Garrett, C. E. Svensson, D. S. Cross, A. B. Garnsworthy, R. Kshetri, J. N. Orce, M. R. Pearson, E. R. Tardiff, H. Al-Falou, R. A. E. Austin, R. Churchman, M. K. Djongolov, R. D'Entremont, C. Kierans, L. Milovanovic, S. O'Hagan, S. Reeve, S. K. L. Sjue, and S. J. Williams, Phys. Rev. Lett. **109**, 042301 (2012).
[27] P. Ujić, F. de Oliveira Santos, M. Lewitowicz, N. L. Achouri, M. Assié, B. Bastin, C. Borcea, R. Borcea, A. Buta, A. Coc,

G. de France, O. Kamalou, J. Kiener, A. Lepailleur, V. Meot, A. Pautrat, M. G. Saint Laurent, O. Sorlin, M. Stanoiu, and V. Tatischeff, Phys. Rev. Lett. **110**, 032501 (2013).

[28] L. J. Broussard, H. O. Back, M. S. Boswell, A. S. Crowell, P. Dendooven, G. S. Giri, C. R. Howell, M. F. Kidd, K. Jungmann, W. L. Kruithof, A. Mol, C. J. G. Onderwater, R. W. Pattie, Jr., P. D. Shidling, M. Sohani, D. J. van der Hoek, A. Rogachevskiy, E. Traykov, O. O. Versolato, L. Willmann, H. W. Wilschut, and A. R. Young, Phys. Rev. Lett. **112**, 212301 (2014).

[29] C. Fontbonne, P. Ujić, F. de Oliveira Santos, X. Fléchard, F. Rotaru, N. L. Achouri, V. G. Alcindor, B. Bastin, F. Boulay, J. B. Briand, A. M. Sánchez-Benítez, H. Bouzomita, C. Borcea, R. Borcea, B. Blank, B. Carniol, I. Čelikovíc, P. Delahaye, F. Delaunay, D. Etasse, G. Fremont, G. de France, J. M. Fontbonne, G. F. Grinyer, J. Harang, J. Hommet, A. Jevremović, M. Lewitowicz, I. Martel, J. Mrazek, M. Parlog, J. Poincheval, D. Ramos, C. Spitaels, M. Stanoiu, J. C. Thomas, and D. Toprek, Phys. Rev. C **96**, 065501 (2017).

[30] B. Fenker, A. Gorelov, D. Melconian, J. A. Behr, M. Anholm, D. Ashery, R. S. Behling, Cohen I. Craiciu, G. Gwinner, J. McNeil, M. Mehlman, K. Olchanski, P. D. Shidling, S. Smale, and C. L. Warner, Phys. Rev. Lett. **120**, 062502 (2018).